A Target Grabbing Strategy for Telerobot Based on Improved Stiffness Display Device

Pengwen Xiong, Xiaodong Zhu, Aiguo Song, *Senior Member, IEEE*, Lingyan Hu, Xiaoping P. Liu, *Senior Member, IEEE*, and Lihang Feng

***Abstract*—Most target grabbing problems have been dealt with by computer vision system, however, computer vision method is not always enough when it comes to the precision contact grabbing problems during the teleoperation process, and need to be combined with the stiffness display to provide more effective information to the operator on the remote side. Therefore, in this paper a more portable stiffness display device with a small volume and extended function is developed based on our previous work. A new static load calibration of the improved stiffness display device is performed to detect its accuracy, and the relationship between the stiffness and the position is given. An effective target grabbing strategy is presented to help operator on the remote side to judge and control and the target is classified by multi-class SVM (supporter vector machine). The teleoperation system is established to test and verify the feasibility. A special experiment is designed and the results demonstrate that the improved stiffness display device could greatly help operator on the remote side control the telerobot to grab target and the target grabbing strategy is effective.**

***Index Terms*—Multi-class SVM (supporter vector machine), teleoperation, target grabbing, stiffness display.**

I. Introduction

As we all know, human-robot interaction plays a quite important role in the area of telerobot [1]−[7]. Haptic interaction between the human operator and telerobot is being widely researched since effective haptic display could help and make the operator more convenient and easier to fulfill remote control tasks, especially some precision contact tasks [8], [9], such as grabbing an unknown target.

Haptic display is classified into two classes [10], one is haptic display in the tangent direction of the touched point, such as texture and friction display, which could be derived or estimated by computer vision system or human vision system [11]−[14]; another is haptic display in the normal direction, such as compliance display and softness display, which definitely cannot be reached by vision system, but is very important to be used to distinguish how hard the object to be grabbed is during the precision contact tasks and how much force the operator should apply. So far, most previous work about target grabbing by a telerobot was focused on the computer vision method and vision system [15]−[17], but vision method is not always competent to provide enough effective information to the operator, and the shortages could be concluded as follows:

1) Even the most advanced computer-vision skill may be affected and limited by the environment light and the nature of object;

2) In some situations, the panorama of the whole object is always hard to get only by computer-vision method;

3) It is contact and force that are the most important points during the grabbing process, and they can't be judged changing and controlled by the computer-vision method.

Especially during the teleoperation with a precision contact grabbing task, stiffness display could be much helpful to the operator on the remote side to increase the safety and stability during the grabbing process. While little research focused on the stiffness display device itself because of the lack of an effective stiffness display interface device with a wide stiffness range from very soft to very hard. An experimental system for measuring planar tissue phantom deformation during needle insertions has been developed and a method for quantifying the needle forces and soft tissue deformations that occur during general needle trajectories in multiple dimensions is proposed in [18]. Those existing PHANToM arm, like some other force feedback data-gloves, are inherently force display interface devices, which are unable to produce large stiffness display of hard object owing to the limitation of output force of the driven motors [19], [20].

In order to solve the precision contact problem, this paper presents a novel target grabbing strategy for telerobot, which is based on improved stiffness display device we designed before [10]. The improved stiffness display interface device, with a small volume and extended function, is made up of a thin

Manuscript received May 31, 2016; accepted October 26, 2016. This work was partially supported by the National Natural Science Foundation of China (61663027, 61325018, 81501560), and the Science and Technology Department of Jiangxi Province of China (20151BAB207050). Recommended by Associate Editor Zhijun Li. *(Corresponding author: Lingyan Hu.)*

Citation: P. W. Xiong, X. D. Zhu, A. G. Song, L. Y. Hu, X. P. P. Liu, and L. H. Feng, "A target grabbing strategy for telerobot based on improved stiffness display device," *IEEE/CAA J. of Autom. Sinica*, vol. 4, no. 4, pp 661−667, Oct. 2017.

P. W. Xiong is with the School of Information Engineering, Nanchang University, Nanchang 330031, China, and also with the School of Instrumentation Science and Engineering, Southeast University, Nanjing 210096, China (e-mail: steven.xpw@ncu.edu.cn).

A. G. Song is with the School of Instrumentation Science and Engineering, Southeast University, Nanjing 210096, China (e-mail: a.g.song@seu.edu.cn).

X. P. P. Liu is with the Department of Systems and Computer Engineering, Carleton University, Ottawa, ON K1S 5B6, Canada, and also with the School of Information Engineering, Nanchang University, Nanchang 330031, China (e-mail: xpliu@sce.carleton.ca).

X. D. Zhu and L. Y. Hu are with the School of Information Engineering, Nanchang University, Nanchang 330031, China (e-mail: xiaohd@email.ncu.edu.cn; hulingyan@ncu.edu.cn).

L. H. Feng is with the Computer Integrated Surgical Systems and Technology Engineering Research Center (CISST ERC), Johns Hopkins University, Baltimore, MD 21218, USA (e-mail: lfeng8@jhu.edu).

Color versions of one or more of the figures in this paper are available online at http://ieeexplore.ieee.org.

Digital Object Identifier 10.1109/JAS.2016.7510256

elastic beam and an actuator to adjust the length of the beam. Under a constant force, the deformation of the beam is proportional to the third power of the beam length. Therefore, we could control the beam length to get the desirable stiffness, which measures the stiffness of a remote object with wide range from very soft to hard, to display on fingertip of human operator. Based on the stiffness display device, a novel target grabbing strategy is presented to provide supportive data and help operator to judge what the object is and to decide how to control to grab the object. The rest of this paper is organized as follows: In Section II, a more flexible and practical stiffness display device is improved and introduced in detail. In Section III, static load calibration of the stiffness display device is extracted and analyzed, and the relationship between the stiffness and the position is given. In Section IV, an effective target grabbing strategy based on the improved stiffness display device is presented and in Section V, multi-class SVM is used to classify the substance of the target and help to verify whether the target is stably handled. Section VI presents our experiment results and Section VII concludes the paper and describes the future work.

II. Improved Stiffness Display Device

We already made a softness haptic display device for human-computer interaction before [10]. However, its size is too large to be carried and it is hard to move on the plane and not convenient to integrate with other equipment for portable use.

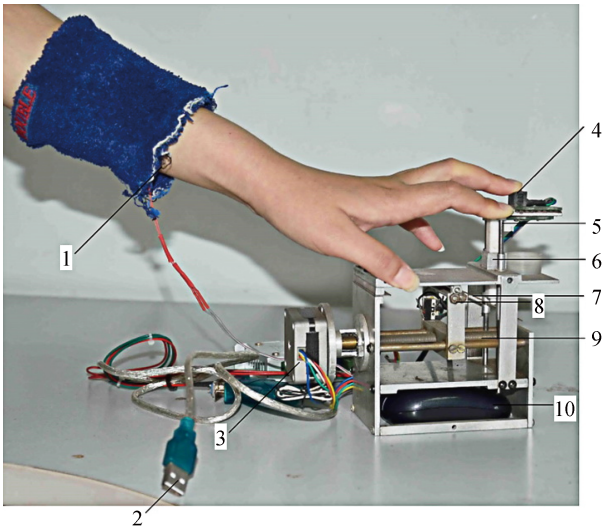

Fig. 1. Improved stiffness display device with vibration motor. 1. vibration motor, 2. USB interface, 3. motor and encoder, 4. touch cap, 5. two protrusive guide poles, 6. position sensor, 7. thin elastic beam, 8. carriage with nut, 9. feed screw, 10. mouse.

Therefore, a small stiffness display device is improved and extended functionally based on the existing device:

1) On the basis of the guaranteed performance, the volume of the device is designed much smaller.

2) A vibration motor is added to display force feedback for operator on the remote side.

3) Two protrusive guide poles which extend to the left and right mouse buttons respectively could be used to input control commands. Therefore, the whole device could take place of the mouse.

4) USB interface is exploited as the mere data interface, it is convenient for plug and play.

As shown in Fig. 1, it is the picture of the improved stiffness display device. In the bottom of the device, a computer mouse is placed, and we could control the left mouse button and right mouse button via the two protrusive guide poles on the top of device, which could be used to control the opening and closing of the gripper. A vibration motor glued on the operator's arm could give the force feedback from the telerobot. The size of the whole device is quite small and convenient for use, about 100 mm long 70 mm wide and 150 mm high. The thin elastic beam was made by spring steel, with the height of 90 mm, the width of 10 mm and the thickness of only 0.3 mm.

According to the principle of the softness display described in [10], the stiffness of the device could be calculated by the formula:

$$k = \rho \frac{1}{l^3} \tag{1}$$

where $\rho = Ebh^3/4$ is the gain of the stiffness, l is the effective length of the thin elastic beam. Here, E is the Young's modulus $E = 200 \times 10^9\,\mathrm{N/m^2}$, and b is the width of the thin elastic beam b = 10 mm, and h is the thickness h = 0.3 mm. So it is easy to calculate with the variable to get the device constant $\rho = 0.0135\,\mathrm{N/m^2}$.

To simplify the calculation, we let $z = 1/l^3$, and substitute it into (1), which could be transformed into a linear function as:

$$k = \rho \cdot z. \tag{2}$$

The relationship between k and l or z is shown in Fig. 2, respectively.

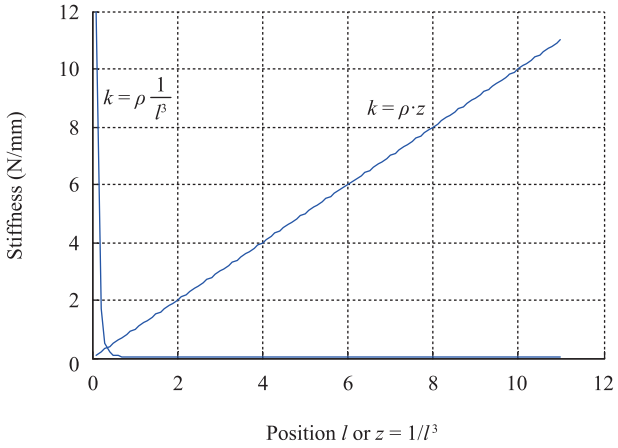

Fig. 2. Transformation of the power function into linear function.

Elastic beam and stiffness display mechanism in the structure inherently determines that the elastic beam has its own shortest effective length and longest effective length to ensure accuracy. With the effective length of the longest $l_{\max}$ and the effective length of the shortest $l_{\min}$

$$\begin{cases} l_{\max} = 81.5\,\mathrm{mm} \\ l_{\min} = 20.5\,\mathrm{mm} \end{cases} \tag{3}$$

substituted to (1), we could get

$$\begin{cases} k_{\max} = 1500.18\,\mathrm{N/mm} \\ k_{\min} = 24.85\,\mathrm{N/mm}. \end{cases} \tag{4}$$

It means that the stiffness display device could reflect stiffness range from 24.85 N/mm to 1500.18 N/mm with comparable accuracy, which is almost enough to display the stiffness of the object in our daily life.

III. Static Load Calibration

After the improved stiffness display device is made, static load calibration is performed as a certain procedure as follows:

1) We pick up a series of feature points, whose coordinates correspond to the current effective length l within the effective range.

2) We successively upload and download weights on the feature points we have selected, and test values of the corresponding strain under different load.

3) The relationship between the output value and the strain could be got and the final characteristic fitting curve of the system could be derived.

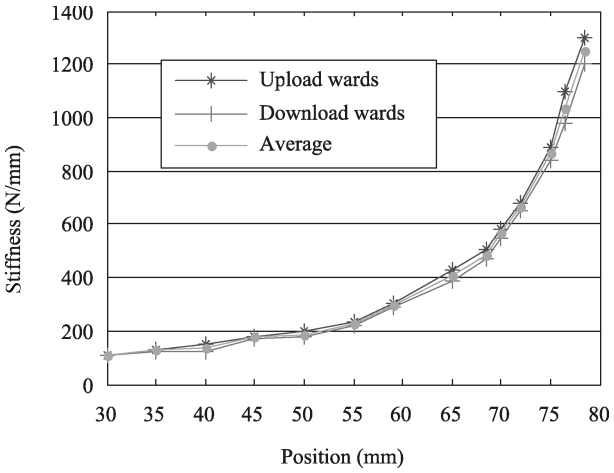

Fig. 3. Results of stiffness calibration.

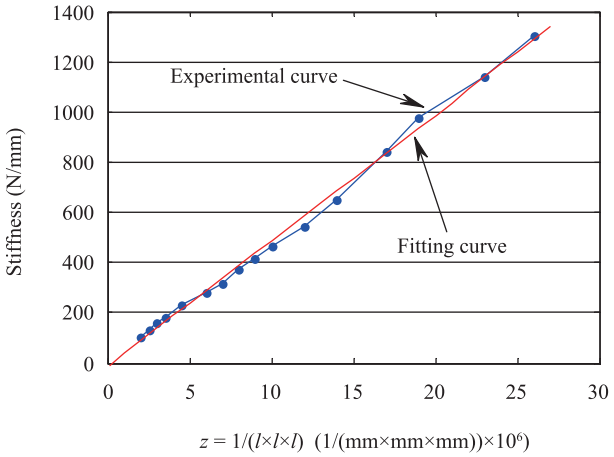

Fig. 4. Fitting curve of characteristic of stiffness.

In the static load calibration experiment, 16 feature points corresponding to the different effective length of the elastic beam are measured, the result is shown in Fig. 3. Then the least square method is used to fit the curve of characteristic of stiffness, which is shown in Fig. 4. The results demonstrate that the improved stiffness display device is able to realize the stiffness display from a virtual environment or telerobot.

IV. Target Grabbing Strategy

Take the tracked mobile robot (TMR) which we have designed in [21] for example, a target grabbing strategy based on the improved stiffness display device is presented.

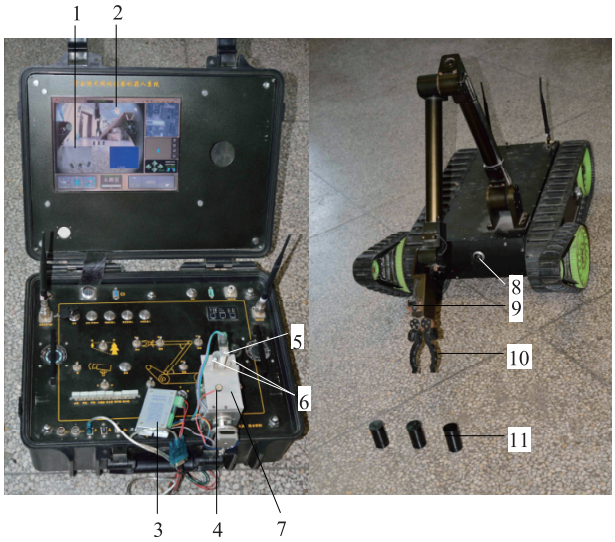

Fig. 5. Teleoperation system for target grabbing. 1. gripper camera display, 2. main camera display, 3. hardware circuit, 4. vibration motor, 5. touch cap, 6. two protrusive guide poles, 7. stiffness display device, 8. main camera, 9. gripper camera, 10. gripper, 11. samples.

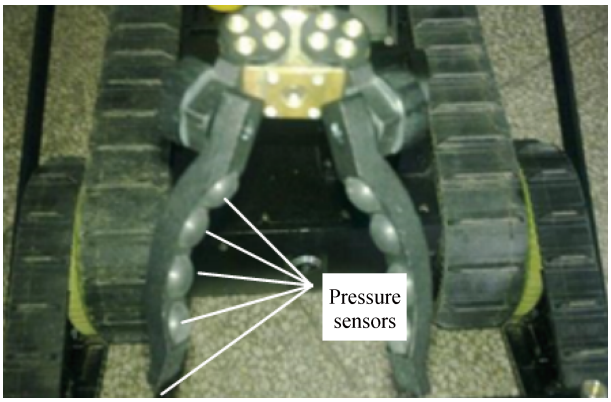

Fig. 6. Pressure sensors distribution on the gripper.

In our previous task, when TMR is well prepared to grab a certain object, it does completely according to the multiple characteristics derived from computer vision, or based on the remote video surveillance. However, there is still some important characteristic which cannot be ascertained only by computer vision, even human vision, such as stiffness of the object and grasping force and so on. So it is quite significant to bring in the small stiffness display device.

Therefore, as shown in Figs. 5 and 6 we establish the teleoperation system for target grabbing. During the teleoperation process, the operator on the operational side controls the command output device on the control box, as shown in Fig. 5,

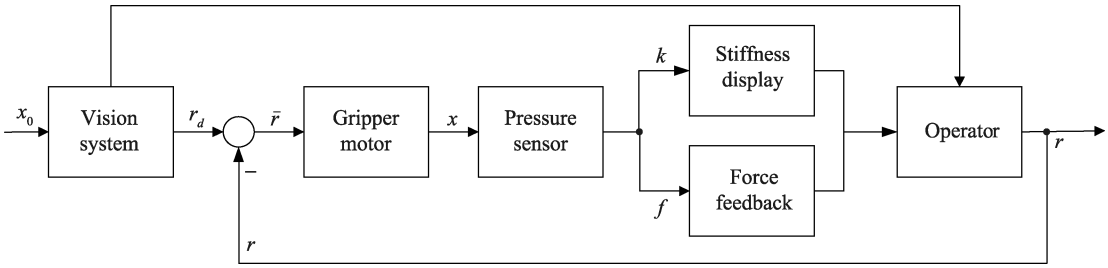

Fig. 7. Target grabbing strategy for telerobot.

and the robot on the remote side will responds with a decided action. After the robot contacts with the object, the sensors placed on the robot detect the useful information from the object, and return the feedback to the control box and provide it to the operator on the operational side.

To succeed to grab a certain object accurately, the extent of the gripper's opening is very important and should be controlled precisely, and the gripper's opening and closing depends completely on the gripper motor. Therefore, it is quite significant to find the appropriate gripper motor displacement.

As shown in Fig. 7, when it is about to control the robot on the remote side to grab a certain object, the gripper loaded on the manipulator with an initial open displacement x_0, is moved to proper position along with the motion of manipulator, an angle r_0 of the gripper motor, which leads the just contact critical position between gripper and object, could be estimated by vision system — it includes computer vision and human vision. Based on the vision system, the operator gives an initial modification value r, and makes the gripper motor work as vector $\bar{r} = r - r_d$. At this moment, gripper starts to extrude the object and the object will produce a tiny deformation x, simultaneously, the pressure sensors on the gripper could detect how much force it is applying.

The formula shows how to choose the best force value as follows:

$$f = \begin{cases} F_0, & F_0 \neq 0 \\ \max\{F_1, F_2, F_3, F_4\}, & F_0 = 0 \end{cases} \tag{5}$$

where F_0 comes from the sensor on the front plane jaw, and it always gets the force firstly and directly during the grabbing task, and it works in most cases; while F_1, F_2, F_3, F_4 is the force obtained from the four sensors placed on the arc jaw, as shown in Fig. 6, and they work only in the situation that the object needs an encompassed mechanism and a closed force to grab. When the encompassed grabbing process happens, the sensor F_0 does not contact with the object, while anyone of the four sensors F_1, F_2, F_3, F_4 may touch the object, and they will not offset each other, and the sensor with most contact will better reflect the object.

The stiffness of the object k could be calculated as follows:

$$k = \frac{f}{\bar{x}'} \tag{6}$$

where $\bar{x}$ is the total deformation under the force f, it could be calculated by r and f.

Then, the operator on the remote side could get the stiffness of the object by touching the touch cap of the improved stiffness display device, as well as the magnitude of force by vibration frequency of vibration motor.

At last, the operator gives a new modification value r, and makes the gripper motor work as the updated vector $\bar{r} = r - r_d$, and turn around and around, until it gets the appropriate gripper motor displacement by the latest r.

V. Grabbing Effect Detection by Multi-class SVM

Detection of the grabbing effect to check whether the target is stably handled by the gripper is very important to the operator on the remote side.

Multi-class SVM (MSVM) [22], [23] is qualified and has a broad use in the classification with several effective vectors, and it could be used to judge what kind of substance the target is, then the operator will decide how to control the gripper next.

A. The Selection of Feature Vectors

The magnitude of force value f is changing all the time during the grabbing process, and the regularity of changing could reflect the difference. Therefore the support vectors are selected based on the magnitude of force value:

1) Sum of gradient squares: $P = \sum_{i=2}^{N} (f_i - f_{i-1})^2$.

This vector shows the changing information of force value, N is the total sampling number of the series.

2) Mean: $A = (1/N) \sum_{i=1}^{N} f_i$.

This variable shows the expectation of the force value series.

3) Variance: $S = (1/(N-1)) \sum_{i=1}^{N} (f_i - \bar{f})^2$.

This variable describes the degree of dispersion of the force value.

4) Maximum: $M = \max_i(f_i)$.

This vector shows the biggest force imposed during the grabbing process.

The feature vector $[P, A, S, M]$ constitutes the support vector x_i, and is the input of the multi-class SVM. Then a training set $T = (x_1, y_1), \ldots, (x_N, y_N)$ is built, where $x_i \in \mathbb{R}^4, y_i = (1, 2, \ldots, n)$, N is the total number of training samples, and n is the number of the classification categories.

B. Multi-Class SVM

The main idea of SVM [24]−[27], as shown in Fig. 8, is to find a decision function $f(x) : X = R^4 \rightarrow Y$ and a classification hyperplane H to make the classification margin big enough and divide the samples clearly from the training set T.

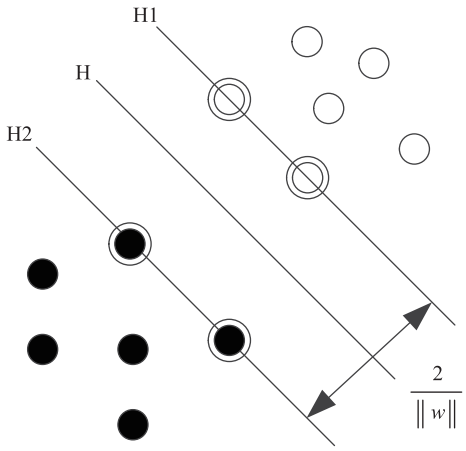

Fig. 8. Classification hyperplane H.

The 1-a-1 method [28], [29] is one of the most popular method of multi-class SVM, which builds a classifier towards every two classes. It leads to $n(n-1)/2$ classifiers if there are n classes and every classifier will train the samples from the two classes.

In order to get the classification hyperplane between class i and class j, the following optimization problem needs to be solved:

$$\min_{\omega^{ij},b^{ij},\xi^{ij}} \frac{1}{2}(\omega^{ij})^T\omega^{ij} + C\sum_t \xi_t^{ij}(\omega^{ij})^T \tag{7}$$

$$(\omega^{ij})^T\Phi(x_t) + b^{ij} \geq 1 - \xi_t^{ij}, \quad \text{if} \quad y_t = i \tag{8}$$

$$(\omega^{ij})^T\Phi(x_t) + b^{ij} \geq \xi_t^{ij} - 1, \quad \text{if} \quad y_t = j \tag{9}$$

$$\xi_t^{ij} - 1 \geq 0, \quad i,j = 1,2,\ldots,n \tag{10}$$

where ω^{ij} is the optimal hyperplane vector between class i and class j, x_t is the tth sample in the sample set X . $\Phi(x_t)$ is higher space, and C is penalty parameter, and the minimum of $(w^i)^T w^i/2$ is the classification margin $2/\|w^i\|$

Radial basis function is applied to calculate inner product in the higher space:

$$K(x_i,x) = \exp\left\{-\frac{\|x-x_i\|^2}{\sigma^2}\right\}, \quad \sigma > 0. \tag{11}$$

The decision function $f(x) = \operatorname{sgn}[(\omega^{ij})^T\Phi(x) + b^{ij}]$ is sign function, and if the result shows x belongs to class i, the statistical variable of class i will add one, otherwise, the statistical variable of class j will add one.

After all of $n(n-1)/2$ classifiers have been applied, the class with the maximum of the statistical value is which x belongs.

VI. Experiment

To make the experiment more effective, we designed three columned samples specially for grabbing experiment, as shown in Fig. 5.

300 samples were made by iron (class 1), rubber (class 2) and sponge (class 3), respectively. The most important thing is that all the samples are painted black and made like a black thin cylinder, and in this case, the experiment candidates couldn't distinguish the samples rely on vision.

180 random samples were picked evenly to conduct the training using multi-class SVM. By grid traverse of the penalty parameter and width parameter of RBF, the best group of the parameter was obtained: $C = 68, \sigma = 1.3$. The remaining 120 samples were checked by the multi-class SVM. The result in Fig. 9 shows that only one sample was classified incorrectly and the accuracy rate is 99.17 %.

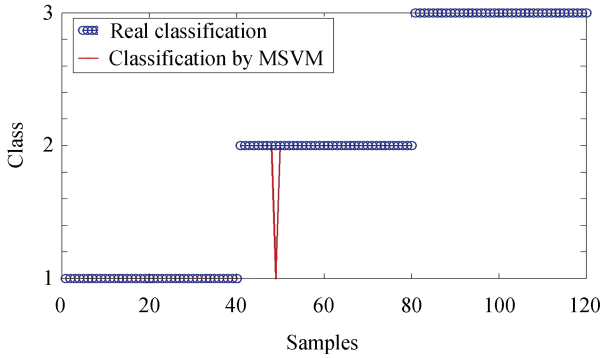

Fig. 9. Classification result by MSVM.

Different grabbing methods were applied in different classes to make sure the object was handled stably. The iron object needs to be clamped by the gripper as well as continuous strong force imposed by the gripper; the rubber object needs to be clamped by the gripper with a bit deformation; the sponge just needs to be caught by the gripper to avoid the case that too much deformation leads to its destruction.

Then, 50 candidates were invited to use our operating platform to perform two groups of experiments. They conduct the first group to snatch up the samples from the 3 classes and move them to another place without the improved stiffness display device, and then the same was continued with the other group after loading the improved stiffness display device.

The result of the experiments is shown in Figs. 10 and 11. In Fig. 10, it is obvious that experiment candidates in Group 2 own a much higher success ratio than the candidates in Group 1.

Fig. 10 shows that failure ratio for the three samples in the series of two group experiments. The sample made by iron was made up of 62 % because experiment candidates always apply a bit less force to grab it in the case of not understanding what they are grabbing, and the force cannot offset the gravity of the iron sample, so it failed and dropped in the middle of movement. Oppositely, sample made by sponge was made up of 35 % because experiment candidates always apply a bit more force to grab it and break the black thin film which packs the sample.

The result of the series of experiments demonstrates that the improved stiffness display device could greatly help operator on the remote side to control the telerobot to grab target with an adequate acquaintance about the stiffness of the target, especially when combined with computer vision system, and the target grabbing strategy is effective in the situation and could be extended.

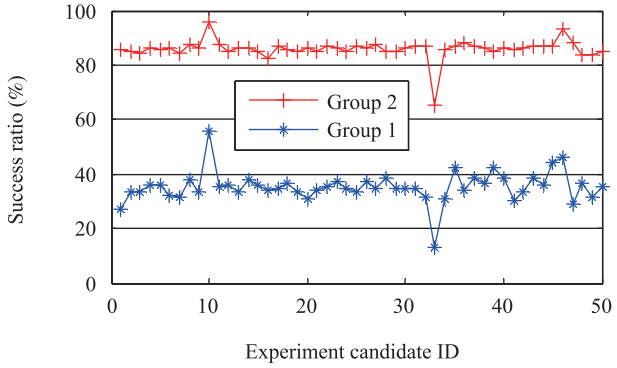

Fig. 10. Success ratio during the experiment candidates.

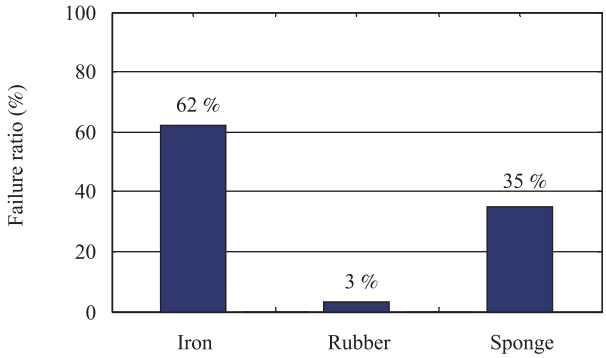

Fig. 11. Failure ratio during different samples.

VII. Conclusion and Future Direction

Based on the previously improved stiffness display device, a more portable stiffness display device with a small volume and extended function is proposed. A new static load calibration of the improved stiffness display device is performed to detect its accuracy, and the relationship between the stiffness and the position is given. An effective target grabbing strategy is presented and the teleoperation system is established to test and verify the feasibility. To make stiffness more evident, the experiment is designed specially and the results demonstrate that the improved stiffness display device could greatly help operator on the remote side control the telerobot to grab target with an adequate acquaintance about the stiffness of the target, and the target grabbing strategy is effective. The future work will focus on the control method of grabbing, especially in the precision contact grabbing problem. Multiple targets recognition under complex environment is also a research point which needs to be figured out.

VIII. Acknowledgment

We need to thank the colleagues from the Key Laboratory of Remote Measurement and Control Technology of Jiangsu Province for their cooperation and kind advice for this work.

References

[1] P. Dario, B. Hannaford, and A. Menciassi, "Smart surgical tools and augmenting devices," *IEEE Trans. Rob. Automat.*, vol. 19, no. 5, pp. 782−792, Oct. 2003.

[2] H. J. Li and A. G. Song, "Virtual-environment modeling and correction for force-reflecting teleoperation with time delay," *IEEE Trans. Ind. Electron.*, vol. 54, no. 2, pp. 1227−1233, Apr. 2007.

[3] W. Qin, Z. X. Liu, and Z. Q. Chen, " Formation control for nonlinear multi-agent systems with linear extended state observer," *IEEE/CAA J. Automat. Sin.*, vol. 1, no. 2, pp. 171−179, Apr. 2014.

[4] Y. N. Yang, C. C. Hua, and X. P. Guan, "Finite time control design for bilateral teleoperation system with position synchronization error constrained," *IEEE Trans. Cybern.*, vol. 46, no. 3, pp. 609−619, Mar. 2015.

[5] C. C. Hua, Y. N. Yang, and P. X. Liu, "Output-Feedback adaptive control of networked teleoperation system with time-varying delay and bounded inputs," *IEEE/ASME Trans. Mechatron.*, vol. 20, no. 5, pp. 2009−2020, Oct. 2015.

[6] Y. N. Yang, C. C. Hua, and X. P. Guan, "Adaptive fuzzy finite-time coordination control for networked nonlinear bilateral teleoperation system," *IEEE Trans. Fuzzy Syst.*, vol. 22, no. 3, pp. 631−641, Jun. 2014.

[7] Y. N. Yang, C. C. Hua, and X. P. Guan, "Finite-time synchronization control for bilateral teleoperation under communication delays," *Robot. Comput. Integr. Manuf.*, vol. 31, pp. 61−69, Feb. 2015.

[8] L. Z. Pan, A. G. Song, G. Z. Xu, H. J. Li, H. Zeng, and B. G. Xu, "Safety supervisory strategy for an upper-limb rehabilitation robot based on impedance control," *Int. J. Adv. Rob. Syst.*, vol. 10, no. 2, pp. 127, Feb. 2013.

[9] A. Bicchi, E. P. Scilingo, and D. De Rossi, "Haptic discrimination of softness in teleoperation: The role of the contact area spread rate," *IEEE Trans. Rob. Automat.*, vol. 16, no. 5, pp. 496−504, Oct. 2000.

[10] S. Aiguo, L. Jia, and W. Juan, "Softness haptic display device for human-computer interaction," *Int. J. Adv. Rob. Syst.*, vol. 5, pp. 257−278, 2008.

[11] X. Wang, N. D. Georganas, and E. M. Petriu, "Fabric texture analysis using computer vision techniques," *IEEE Trans. Instrum. Meas.*, vol. 60, no. 1, pp. 44−56, Jan. 2011.

[12] D. Copeland and J. Finlay, "Identification of the optimum resolution specification for a haptic graphic display," *Interact. Comput.*, vol. 22, no. 2, pp. 98−106, Mar. 2010.

[13] J. Wu, L. Y. Li, R. Q. Yan, D. J. Ni, and W. Liu, "Experimental study on virtual texture force perception using the JND method," *Int. J. Adv. Rob. Syst.*, vol. 9, pp. 63, Jun. 2012.

[14] A. Oonsivilai and N. Meeboon, "Silk texture defect recognition system using computer vision and artificial neural networks," in *Proc. 2nd International Congress on Image and Signal Processing*, Tianjin, China, 2009, 1−4.

[15] H. Fujimoto, L. C. Zhu, and K. Abdel-Malek, "Image-based visual servoing for grasping unknown objects," in *Proc. 26th Annu. Confjerence of the IEEE Industrial Electronics Society*, Nagoya, Japan, vol. 2, pp. 876−881, 2000.

[16] M. Trabelsi, N. Aitoufroukh, and S. Lelandais, "Improvements of object grabbing method by using color images and neural networks classification," in *Proc. 32nd Conf. IEEE Industrial Electronics*, Paris, France, 2006, pp. 3922−3927.

[17] L. Bodenhagen, D. Kraft, and P. E. Hotz, "Learning to grasp unknown objects based on 3D edge information," in *Proc. 2009 IEEE International Symposium on Computational Intelligence in Robotics and Automation*, Daejeon, Korea, 2009, pp. 421−428.

[18] S. P. DiMaio and S. E. Salcudean, "Needle insertion modeling and simulation," *IEEE Trans. Rob. Autom.*, vol. 19, no. 5, pp. 864−875, Oct. 2003.

[19] T. H. Massie and J. K. Salisbury, "The PHANToM haptic interface:

A device for probing virtual objects," in *Proc. ASME Winter Annu. Meeting: Dyn. Syst. and Contr.*, vol. 55, pp. 295−300, 1994.

[20] G. C. Burdea, "Haptics issues in virtual environments," in *Proc. Computer Graphics International*, Geneva, Switzerland, 2000, pp. 295−302.

[21] Y. Guo, A. G. Song, J. T. Bao, H. R. Tang, and J. W. Cui, "A combination of terrain prediction and correction for search and rescue robot autonomous navigation," *Int. J. Adv. Rob. Syst.*, vol. 6, no. 3, pp. 207−214, Sep. 2009.

[22] C. W. Hsu and C. J. Lin, "A comparison of methods for multiclass support vector machines," *IEEE Trans. Neural Netw.*, vol. 13, no. 2, pp. 415−425, Mar. 2002.

[23] K. Englehart, B. Hudgin, and P. A. Parker, "A wavelet-based continuous classification scheme for multifunction myoelectric control," *IEEE Trans. Biomed. Eng.*, vol. 48, no. 3, pp. 302−311, Mar. 2001.

[24] C. J. C. Burges, "A tutorial on support vector machines for pattern recognition," *Data Min. Knowl. Discov.*, vol. 2, no. 2, pp. 121−167, Jun. 1998.

[25] M. A. Hearst, S. T. Dumais, E. Osuna, J. Platt, and B. Scholkopf, "Support vector machines," *IEEE Intell. Syst. Their Appl.*, vol. 13, no. 4, pp. 18−21, Jul.−Aug. 1998.

[26] O. Chapelle, V. Vapnik, O. Bousquet, and S. Mukherjee, "Choosing multiple parameters for support vector machines," *Mach. Learn.*, vol. 46, no. 1−3, pp. 131−159, Jan. 2002.

[27] C. Huang, L. S. Davis, and J. R. G. Townshend, "An assessment of support vector machines for land cover classification," *Int. J. Remote Sens.*, vol. 23, no. 4, pp. 725−749, Feb. 2002.

[28] C. H. Q. Ding and I. Dubchak, "Multi-class protein fold recognition using support vector machines and neural networks," *Bioinformatics*, vol. 17, no. 4, pp. 349−358, Apr. 2001.

[29] G. M. Foody and A. Mathur, "A relative evaluation of multiclass image classification by support vector machines," *IEEE Trans. Geosci. Remote Sens.*, vol. 42, no. 6, pp. 1335−1343, Jun. 2004.

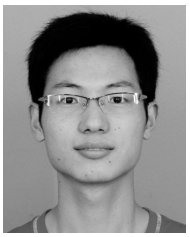

Pengwen Xiong received the B.S. degree from North University of China in 2009, and Ph.D. degree in instrumentation science and technology from Southeast University, China, in 2015. He visited Laboratory for Computational Sensing and Robotics, Johns Hopkins University from 2013 to 2014. He is currently a lecturer at the School of Information Engineering, Nanchang University. His research interests include human robot interaction, robotic sensing and controlling.

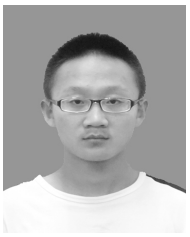

Xiaodong Zhu received the B.S. degree in automation from Nanchang University in 2016, and is currently a master student in control engineering at the School of Information Engineering, Nanchang University. His research interests include human robot interaction, computer simulation and data analysis.

Aiguo Song received the B.S. degree in automatic control in 1990, the M.S. degree in measurement and control in 1993 from Nanjing Aeronautics and Astronautics University, Nanjing, China, and the Ph.D. degree in measurement and control from Southeast University, Nanjing, in 1996. From April 2003 to April 2004, he was a Visiting Scientist with the Lab for Intelligent Mechanical Systems, Northwestern University, Evanston, IL, USA. He is currently a Professor with the Department of Instrumentation Science and Engineering, Southeast University. His current research interests include haptic display and teleoperation robot.

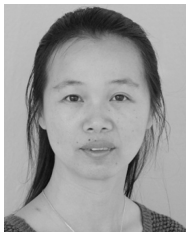

Lingyan Hu received the Ph.D. degree from Nanchang University in 2011. She is currently a Professor in School of Information Engineering, Nanchang University, Nanchang, China. Her current research interests include teleoperation systems, haptic control and virtual surgery system.

Xiaoping P. Liu received the B.Sc. and M.Sc. degrees from Northern Jiaotong University, Beijing, China, in 1992 and 1995, respectively, and the Ph.D. degree from the University of Alberta, Edmonton, AB, Canada, in 2002. He is currently a Canada Research Chair Professor with the Department of Systems and Computer Engineering, Faculty of Engineering and Design, Carleton University, Ottawa, ON, Canada. His research interests include interactive networked systems and teleoperation, robotics, intelligent systems, haptics, micromanipulation, context-aware intelligent networks, and their applications to biomedical engineering.

Lihang Feng received the B.S. degree in flight vehicle design and engineering from Nanjing University of Aeronautics and Astronautics, China, 2009. He is currently a visiting Ph.D student in Laboratory for Computational Sensing and Robotics, Johns Hopkins University, Baltimore, MD 21218, USA. He is also a Ph.D candidate in instrumentation science and technology, Southeast University, China. His research interests include sensing technology, robotics design and modeling.